Supporting Information

Hierarchical configuration of $NiCo_2S_4$ nanotube@ Ni-Mn layered double hydroxide arrays/three-dimensional graphene sponge as electrode materials for high-capacitance supercapacitors

Houzhao Wan[a, b], *Jia Liu*[a], *Yunjun Ruan*[a], *Lin Lv*[a], *Lu Peng*[a], *Xiao Ji*[a], *Ling Miao*[a], *Jianjun Jiang*[a]*

[a]School of Optical and Electronic Information, Huazhong University of Science and Technology, Wuhan 430074, China

[b]Hubei Collaborative Innovation Center for Advanced Organic Chemical Materials, Faculty of Physics and Electronic Science, Hubei University, Wuhan 430062, China

E-mail: jiangjj@mail.hust.edu.cn; Tel.: +86-27-87544472, Fax: +86-27-87544472

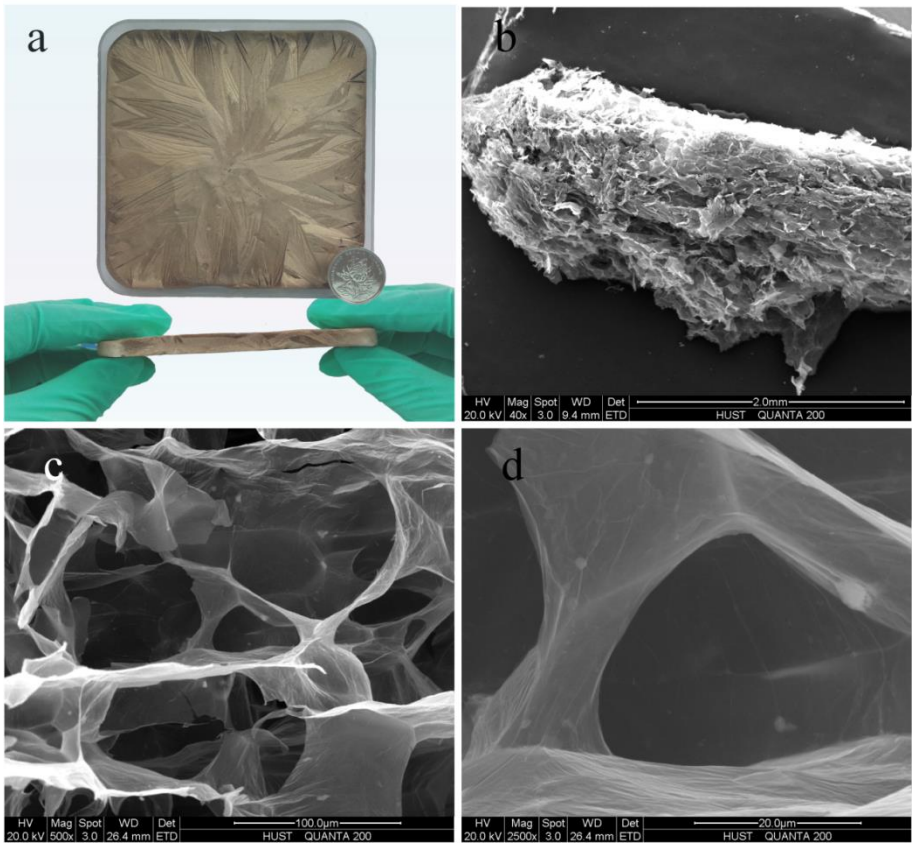

Figure S1 (a) Physical picture of the graphene oxide sponge. (b) Low magnification image of the GOS. (c, d) SEM images of GOS.

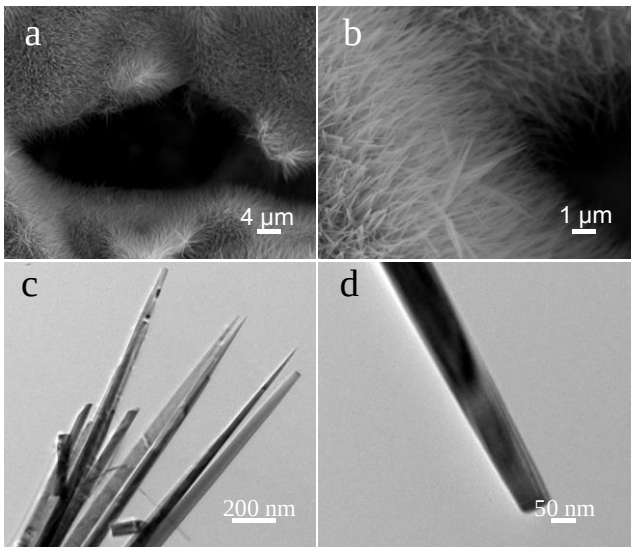

Figure S2 (a, b) SEM and (c ,d) TEM images of Ni-Co-salt precursor nanowire arrays/GS.

the XRD pattern of $NiCo_2S_4$ nanotubes/graphene sponge was shown in Figure S3a according to your comment. The broad peaks with low intensity indicate the poor crystallization of the sample. The diffraction peaks at 26.8 º, 31.5 º, 38.1 º, 47.4 º, 50.4 º and 55.2 ºcorresponding to the respective (220), (311), (400), (422), (511) and (440) planes of the nanostructured cubic type $NiCo_2S_4$ (JCPDS 20-0782). The diffraction peaks show a similar XRD pattern with the cubic Co_3S_4 (JCPDS Card no. 75-1561), except a slight shift of the diffraction peaks towards to the low angle direction, which can further confirm that the substitution of Co ions by Ni ions only slightly changes the lattice parameters while maintains the crystal structure. Two other diffraction peaks at 29.9 ºand 52.1 ºhave the same diffracted angle with the (311) and (440) plane diffraction of Co_9S_8 (JCPDS 65-6801). The substitution of Co ions by Ni ions does not change the crystal structure of the Co-based nanocrystal, which can be proved by the XRD patterns of Ni, Co-based precursor and the $NiCo_2S_4$. According to the element ratio obtained from the XRF test (Figure S3b), the sample is almost solely constituted by $NiCo_2S_4$.

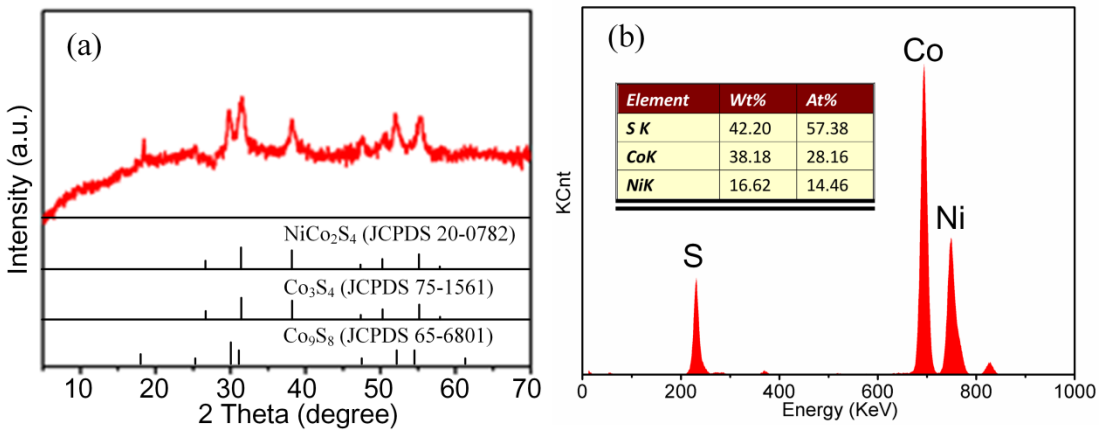

Figure S3 (a) XRD pattern of the $NiCo_2S_4$ nanotubes/graphene sponge. (b) XRF spectrum of the $NiCo_2S_4$ nanotubes/graphene sponge.

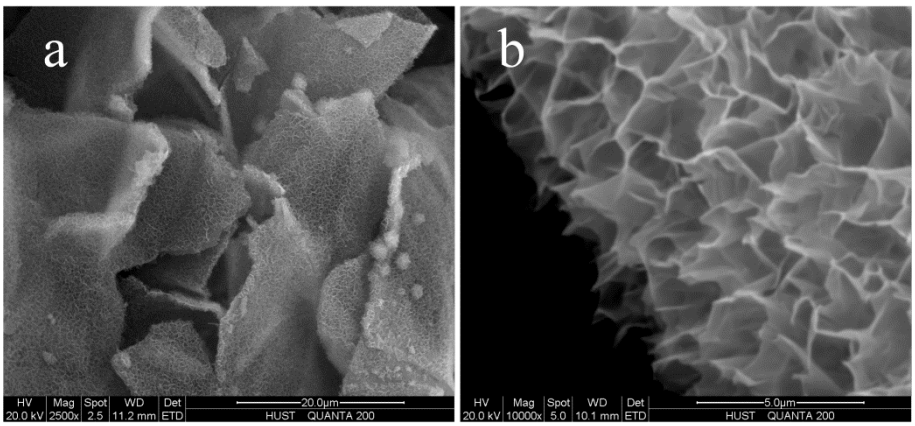

Figure S4 (a, b) SEM images of the Ni-Mn LDH/GS.

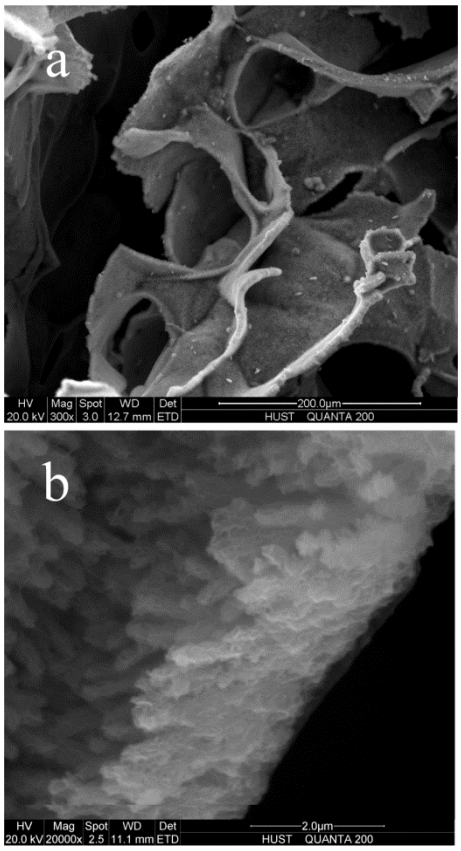

Figure S5 (a, b) SEM images of the $NiCo_2S_4$@ Ni-Mn LDH /GS.

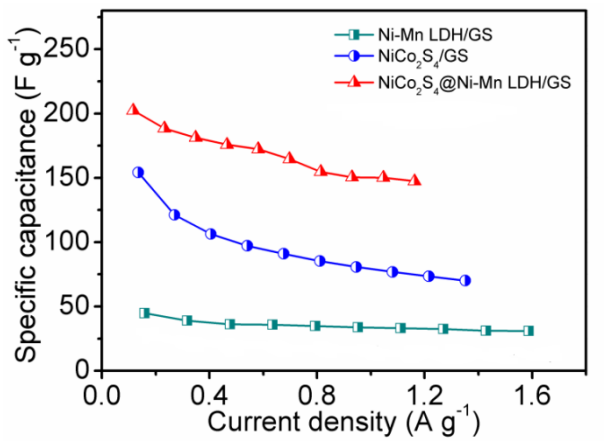

Figure S6 Cap of the electrodes as a function of current density.

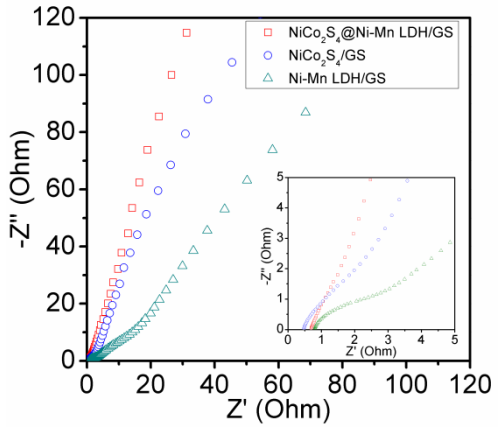

Figure S7 Nyquist impedance plots of the Ni-Mn LDH/GS, $NiCo_2S_4$/GS and $NiCo_2S_4$@ Ni-Mn LDH /GS with frequency ranging from 100 kHz to 0.1 Hz.

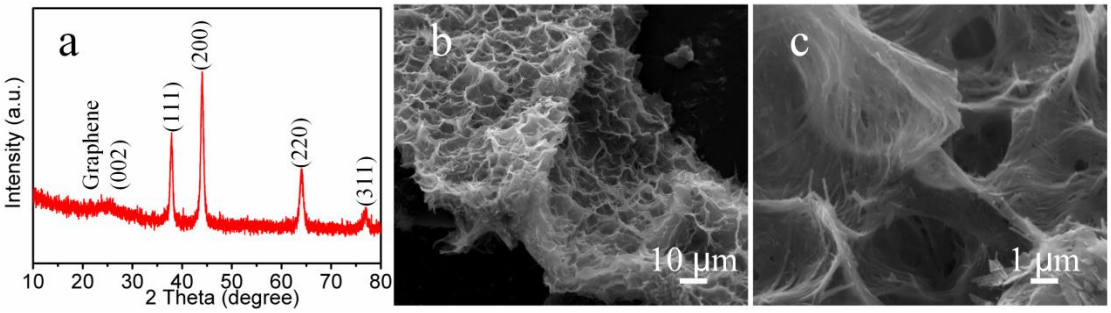

Figure S8 (a) XRD pattern and (b, c) The SEM images of the VN/GS.

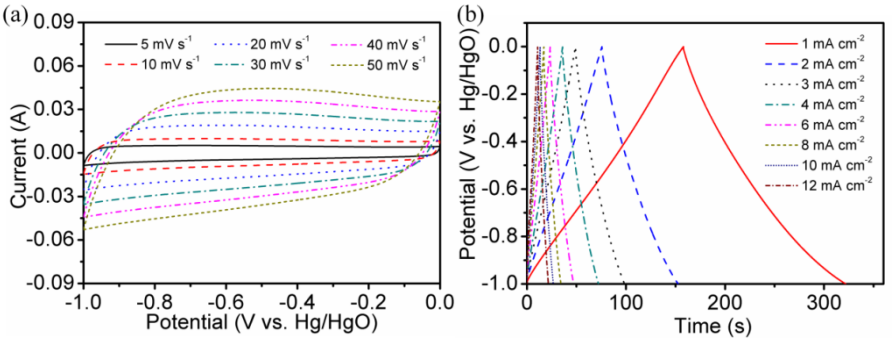

Figure S9 (a, b) CV curves and galvanostatic charge–discharge curves of VN/GS.

The $NiCo_2S_4$@Ni-Mn LDH/GS//VN/GS asymmetric supercapacitor was reassembled according to the formula (S1) and (S2):

$$q = C \times \Delta V \times m \quad \text{(R1)}$$

$$\frac{m_+}{m_-} = \frac{C_- \Delta V_-}{C_+ \Delta V_+} \quad \text{(R2)}$$

Figure S10 compares the CV curves of $NiCo_2S_4$@Ni-Mn LDH/GS and VN/GS electrodes in a three-electrode cell with 6 M KOH aqueous electrolyte at a scan rate of 5 mV s^{-1}. The stable potential range is between −1.0 and 0 V for VN/GS electrode and between -0.1 and 0.6 V for $NiCo_2S_4$@Ni-Mn LDH/GS electrode. The cell voltage can be expressed as the sum of the potential ranges of two electrodes. Figure S10b shows the potential–time curves of the individual electrodes at a current density of 5 mA cm^{-2}. So the mass ratio between the electrodes is balanced to about 1:2.7 according to discharge time.

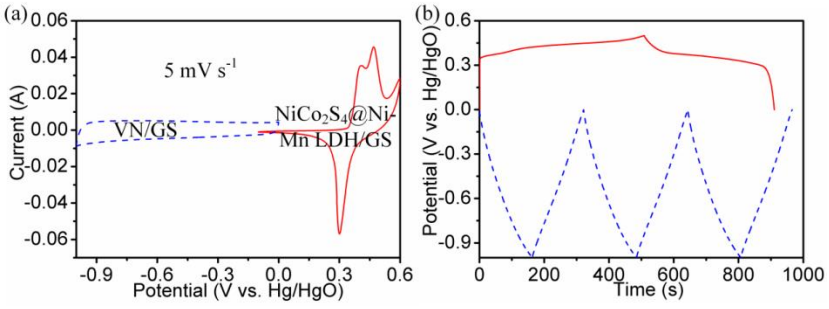

Figure S10 (a) CV curves of $NiCo_2S_4$@Ni-Mn LDH/GS and VN/GS electrodes in a three-electrode cell with 6 M KOH aqueous electrolyte at a scan rate of 5 mV s^{-1}. (b) The potential–time curves of the individual electrodes at a current density of 5 mA cm^{-2}.

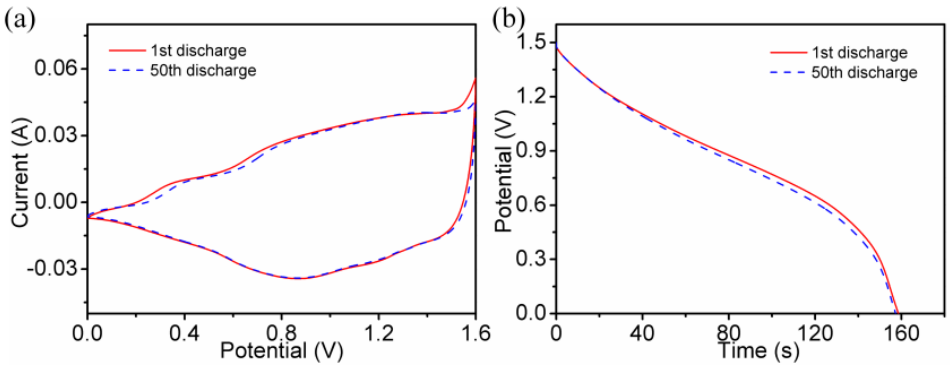

Figure S11 (a) CV curves and (b) galvanostatic discharge curves of the asymmetric device after bending 1st and 50th.

Figure S12 (a) Flexible solar cells charge to the FASC, Charging voltage of 2.729V, (b) Flexible solar cells light LED without FASC, (c) Flexible solar cells light LED with FASC, (d) Our FASC light LED without flexible solar cells.